ISSN: 0067-2904

The Potential of Hybrid Data Integration Approaches Based UAV-SfM Photogrammetry in Identifying New Archaeological Features in The Archaeological UR Site

Alaa Sh. Jaber*[1], Fanar M. Abed[2]
[1]*Department of Surveying Engineering, College of Engineering, University of Baghdad, Baghdad, Iraq*
[2]*Honorary member of the University of Exeter, Exeter, UK*

Received: 7/3/2023 Accepted: 23/7/2023 Published: 30/8/2024

Abstract

Structure-from-Motion (SfM) Photogrammetry-based unmanned aerial vehicles (UAV) are considered one of the most effective non-destructive techniques to detect features in archaeology. However, relying on only standalone-based photogrammetric approaches is not always valid in revealing new archaeological features and monuments. This study aims to verify the efficiency of the integration-based methodologies of SfM photogrammetry products to improve the detection of new archaeological features in the non-excavated regions of the archaeological site of Ur, south of Iraq. The methodology proposes an automatic workflow to extract 3D topographic models such as Digital Terrain Model (DTM) by Agisoft Metashape (MS) software and orthomosaic images as standard products for UAV-photogrammetry. These have delivered the following Structure-from-Motion and Multi-View Stereo (SfM-MVS) algorithms using an optimized flight planning, data capturing, and data processing pipeline. Stand-alone raster images derived from photogrammetry, such as (slope images, hill shade rasters, etc.), have limitations in archaeology compared to hybrid raster images in detecting covered and unrevealed features. The methodology focuses on fusing multiple rasters extracted from DTM using the QGIS software package analysis tools to detect features that may never be detected from single standalone image rasters. This is because combining multiple rasters of different parameters may highlight new potential features such as paths, temples, etc. The results findings revealed that the fusion methodology of raster images obtained from UAV-SfM Photogrammetry through its standard products and using high precision settings could successfully help to identify many new archaeological features in the undiscovered site in Ur, such as walls and houses, which may date back to the late periods of Ur. The results concluded that this enhances the role of photogrammetry and remote sensing techniques as non-destructive excavation tools to provide a rich database for archaeologists for further analysis and interpretation of undiscovered archaeological sites without destruction. Many new archaeological features were also revealed, and a general digital map of the site was prepared. It also prompts a review of the settlement theories in previous studies in the ancient city of UR and the documentation of excavated archaeological ruins.

Keywords: Remote sensing; UAV-Photogrammetry; Integration approaches; Raster images; Visual analysis, archaeological features.

*Email: alaa.jaber1512m@coeng.uobaghdad.edu.iq

الكشف عن السمات الاثرية المحتملة في اور على اساس المسح التصويري للطائرات بدون طيار

علاء شعيل جابر[1]*, فنار منصور عبد [2]

[1]قسم هندسة المساحة, كلية الهندسة, جامعة بغداد, بغداد, العراق

[2]عضو فخري في جامعة إكستر ، إكستر ، المملكة المتحدة

الخلاصة

تعتبر المركبات الجوية بدون طيار (UAV) القائمة على القياس التصويري من خوارزميات الهيكل من الحركة (SfM) واحدة من أهم التقنيات غير المدمرة المستخدمة للكشف عن المعالم في المواقع الأثرية. تهدف هذه الدراسة إلى التحقق من كفاءة منتجات القياس التصويري مع خوارزميات(SfM) القياسية في الكشف عن المعالم الأثرية الجديدة في موقع أور الأثري في المنطقة الجنوبية من العراق. تقترح المنهجية سير عمل تلقائي لاستخراج نموذج طبوغرافي ثلاثي الأبعاد كنموذج التضاريس الرقمي (DTM) وصور متعامدة كمنتجات قياسية في القياس التصويري للطائرات بدون طيار. تم تطبيق ذلك باتباع خوارزميات الهيكل من الحركة واستيريو متعدد العرض (SfM–MVS) وباستخدام خط أنابيب محسن لتخطيط الرحلة ومعالجة البيانات. الصور النقطية المستقلة المشتقة من القياس التصويري مثل (صور المنحدرات ، خطوط التلال النقطية ، وما إلى ذلك) ، لها قيود في علم الآثار مقارنة بالصور النقطية المدمجة والصور النقطية الهجينة في اكتشاف الميزات المدفونة وغير المكتشفة. تركز المنهجية على دمج البيانات النقطية المتعددة المستخرجة من DTM لاكتشاف الميزات التي قد لا يتم اكتشافها مطلقًا من صورة نقطية فردية مستقلة. هذا لأن الجمع بين البيانات النقطية المتعددة من المعلمات المختلفة قد يبرز ميزات محتملة جديدة مثل المسارات والمعابد وما إلى ذلك. كشفت النتائج أن منهجية دمج الصور النقطية التي تم الحصول عليها من القياس التصويري للطائرات بدون طيا رمع خوارزميات (SfM) من خلال منتجاتها القياسية واستخدام إعدادات عالية الدقة يمكن أن تساعد في تحديد العديد من الميزات الأثرية الجديدة في الموقع غير المكتشف في أور مثل ، معالم الجدران أو المنازل ، والتي قد تعود إلى الفترات المتأخرة من حكم أور. هذا يعزز دور المسح التصويري وتقنيات الاستشعار عن بعد كأدوات حفر غير مدمرة لتوفير قاعدة بيانات غنية لعلماء الآثار لمزيد من التحليل والتفسير للمواقع الأثرية غير المكتشفة دون تدمير. كما أنه يدفع إلى مراجعة نظريات الاستيطان في الدراسات السابقة في مدينة أور القديمة، وكذلك توثيق الآثار الأثرية المحفورة.

1. Introduction

Recent developments in geophysics and Remote Sensing (RS) techniques (such as photogrammetry, Ground Penetrating Radar (GPR), and laser scanning) have had a significant influence on scientific understanding and knowledge of archaeological sites [1], [2]. The actual added value of UAV-based photogrammetry is to reduce flight altitudes to a minimum if compared to other platforms, in addition to using Computer Vision (CV) techniques like the Structure- from-Motion algorithm and the Stereo Multi-View (SfM-MVS) to rely on automatic processing [3] entirely. Dense point clouds may be produced using photogrammetry, which is particularly useful for making highly accurate 3D models [3]. Visual image analysis of photogrammetric products such as DTMs is a powerful tool to examine, analyze, and detect archaeological features [4].

Visualization products such as (hillshade, slopes, aspects, etc.) can be computed from 3D topographical models, which still form the foundation of commonness archaeological investigations of photogrammetric data [5]. [6] revealed that profile curvature maps with hill-

shading can successfully increase topographic details through cartography as it may detect variations in slope gradients of as small as 0.5°. These findings have been delivered based on a UAV-SfM photogrammetric dataset collected in southwestern Montana in the Tobacco Root Mountains. After that, [7] used hillside overlay methods to interpret Digital Elevation Model (DEM) and revealed previously undiscovered monuments as the remains of a moat and fortification in 1755 densely forested regions in Canada. Later, [8] considered openness an ideal tool for mapping and identifying monuments by airborne Lidar-derived DTM in two different archaeological sites in Austria and Stockholm. Openness is not subject to directional bias, in contrast to other shading techniques, and the relief characteristics underscore that the results are not skewed horizontally. On the other hand, [5] worked on improving visualization outcomes by Combining various relief visualization products based on a variety of methods (E.g., gloss, dodge, overlay, and multiply) on different sites (Campeche, Mexico, Netherlands, Slovenia) using lidar data. So, allowing the presentation of many topographical elements in a single (improved) image can make tiny topographical elements more visible and easier to see and recognize using a criterion of good visualization.

Later, in Beaufort County in South Carolina, [9] a mound and a fresh shell ring were discovered by applying properties of slope and aspect images. However, a shade-free relief Red Relief Image Map (RRIM) map was recommended. As for the most powerful visual analysis to use, [4] conducted research to determine the effectiveness of several visual analytic approaches developed from the SfM-MVS methodologies in identifying archaeological features in the ancient Babylon City, the center of the ancient Babylonian culture in Iraq. They found that integrated datasets SSD (by merging the Digital Surface Model (DSM), Differential openness, and Sky View Factor (SVF) raster) and RRIM can significantly improve discovery at the archaeological site, corroborating the initial findings of the independent approaches. [10], [11] following this, UAV-photogrammetry was used as a primary tool in this research to draw attention to automatic technique and its contribution to archaeology through utilizing digital advancements of SfM-MVS photogrammetry products as a standalone or integrated product to improve archaeological discoveries worldwide and particularly in non-excavated sites in Iraq.

2. Materials and Methods

The SfM-MVS algorithms allow 3D scenes to be reproduced from images through three main phases: point capture and recovery, surface reconstruction, and texture mapping. The results may be exported as 3D models, dense or sparse point clouds, and orthomosaic by (MS) software for post-processing to reveal potential archaeological features and artifacts [12], [13]. Therefore, this section illustrated the methods implemented to bring results to the target accuracy, starting from good planning and preparation of data acquisition, data collection, and processing, strict procedures followed to deliver the base data DTM to be analyzed, new rasters produced for potential archaeological detection following careful selection of image parameters. The section introduced a brief introduction about the study site and materials utilized.

2.1. The Study Area

Archaeologists recognized that the cradle of civilization originated from southern Mesopotamia, particularly Ur, the capital of the most famous governing Sumerian dynasties, and was established in the fourth millennium B.C. (or maybe before)[14]. Ur dominated the other Sumerian city-states, such as Larsa, Isin, and Eshnunna, and extended to upper Mesopotamia far north through dynasties three (Ur I, Ur II, Ur III) [15] www.ur-online.org. Ur (or "Tell el-Muqayyar") is in the southern Iraqi province of Thi Qar. It is situated around

15 km west of Nasiriyah city (30˚ 57′46″ Latitude, 46˚ 6′15″ Longitude), while the Imam Ali Air Base surrounds the Ur city in the shape of a crescent starting from the southeast to the southwest of the site. At the same time, the other side is surrounded by farmland and separate homes for some farmers. Ur was identified in 1854, but the regular scientific excavations started with a joint expedition led by Sir Leonard Woolley of Pennsylvania University and the British Museum in early 1922[14], Figure (1).

Figure 1: The ancient Ur in southern Iraq is shown in a UAV image on the right and the map of Iraq on the left.

2.2. Data Acquisition

The most challenging aspect of field operations is image capturing [16] because it requires preparing and monitoring many parameters that may significantly affect the accuracy and quality of the results. Consider lighting factors (sun's angle during image capturing), appropriate weather conditions, and establishing a network from the Ground Control Points (GCPs). In this study, fieldwork begins with the distribution of 12 GCPs over the site area (~430 ha). Figure (2) as the break-even points of the distribution of Von Gruber [17], [18].

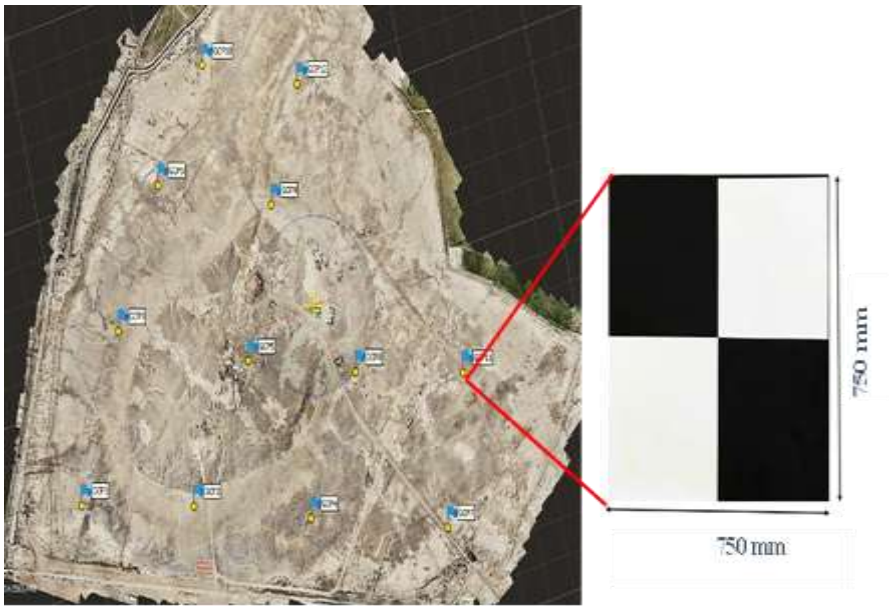

Figure 2: GCP distribution at the study site.

Real-time kinematic positioning (RTK) mode was employed with the Global Navigation Satellite System (GNSS) receiver (Topcon GR-3) to observe the 3D coordinates of these objects at the location, Figure (3). With the EGM08 geoid model, the height is represented as Mean Sea Level (MSL), and the horizontal coordinates system is UTM Zone 38N (World Geodetic System 1984, WGS84).

Figure 3: Observations methods static and (RTK) by GNSS receiver.

The static observation method was employed to measure a local reference station by Differential Global Positioning System (DGPS) for more than 2 hrs. The spatial resolution of the local reference station after post-processing was (Station Longitude (East) (0.012 m), Latitude (North) (0.009 m), Ellipsoidal Height (Up) (0.036m). The more comprehensive and detailed the flight planning, the more effective it is to obtain data of the highest quality and accuracy, allowing photogrammetric solutions to reconstruct 3D models [19] fully automatically.

In this study, a flight plan was developed using the Pix4D capture application, Figure (4), to ensure complete site coverage. The flight was planned using the dual grid method following computed flight parameters to collect the photographic data as illustrated in equations (1 to 8) [19]–[22], Table (1).

$$\mathrm{AGL}_1 = \frac{f \times GSD \times HR}{SW} \quad (1)$$

$$\mathrm{AGL}_2 = \frac{f \times GSD \times VR}{SH} \quad (2)$$

where AGL: stands for the flight altitude over ground level (m); GSD: Ground Sampling Distance (m/pixel); f: for the focal length; SH: for the sensor height; SW: for the sensor width; HR, VR: for the sensor's horizontal and vertical resolutions; (px).

$$GSD = \frac{sensor\ width \times flying\ \ hight \times 100}{focal\ lenght \times image\ width} \quad (3)$$

$$End\ Lap(PE) = \frac{G-B}{G} \times 100 \quad (4)$$

$$Side\ Lap(PS) = \frac{G-W}{G} \times 100 \quad (5)$$

$$UAV\ speed\ (m/s) = \frac{GSD \times (\delta)\ maximum\ motion\ blur}{(lt)\ the\ shutter\ speed} \quad (6)$$

$$SP = \frac{Image\ coverage\ (W)\ x\ (100 - amount\ of\ side\ lap)}{100} \quad (7)$$

Where SP is the distance between flight lines.

$$Number\ of\ flight\ lines\ (NFL) = (WIDTH\ /\ SP) + 1 \quad (8)$$

where G is the dimension of the ground square covered by a single vertical photograph, B is the air base or distance between exposure stations of a stereo pair, and W is the spacing between adjacent flight lines.

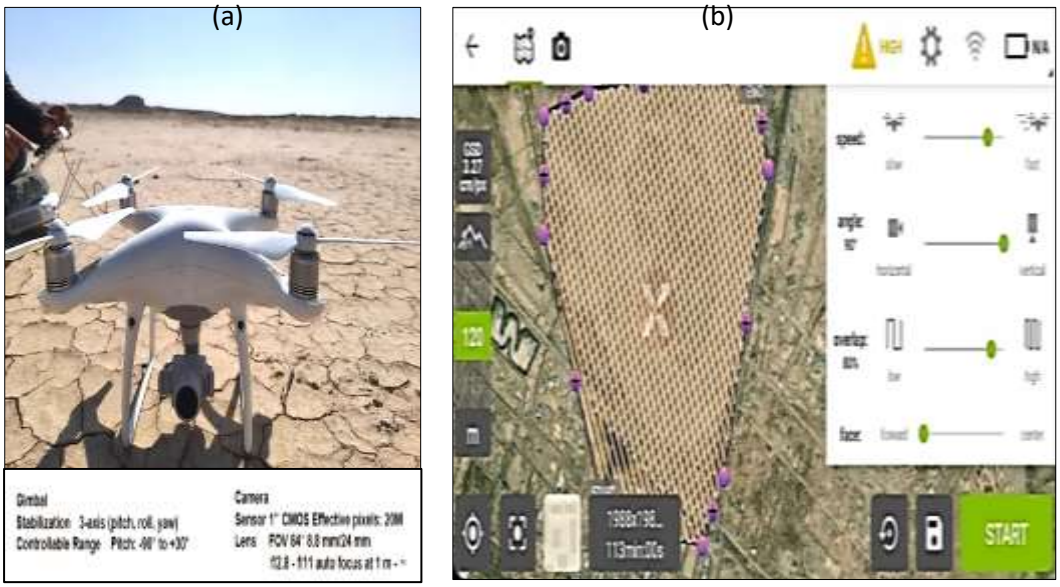

Figure 4: (a) The DJI Phantom 4 UAV was deployed to gather data in the study area;(b) Flight plan settings in the Pix4Dcapture in (7308) images.

Table 1: The UAV flight settings were used for collecting the photogrammetric data.

Parameters	Settings
Flying altitude	120 m
Overlap and side lap	80%, and 70%, respectively
Flightline	91 lines
GSD	3.27 cm

2.3. Data Processing and Modeling

Before starting the implementation of 3D data reconstruction, the filtering process was applied to remove the distorted images that suffer from poor overlap ratios resulting from wind activity and high contrast in the terrain. Then after, the raw images were pre-processed by enhancing the brightness and contrast of the images, which can reduce the impact of shadows and simulate realistic colors and obtain high details, which would enable SfM methods to extract common features in the images, which leads to better alignment, grids, and textures, Figure (5). The Agisoft Metashape Professional (MS) software (paid version) was used to process the taken images (www.agisoft.com) to produce photorealistic 3D models.

MS features the highest levels of automation; however, it provides manual processing control

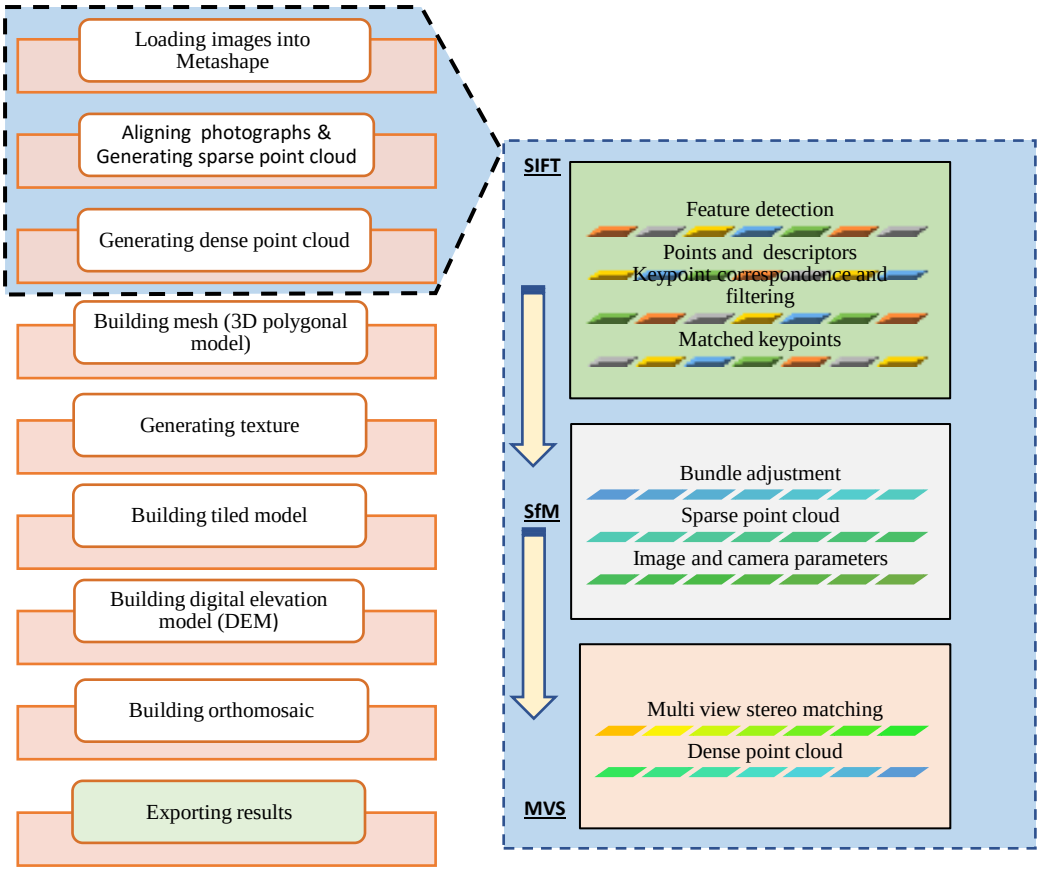

and deals with the widest variety of data types with high reliability.

Figure 5: Schematic workflow for data processing in MS software with SfM-MVS algorithm.

The alignment process was fully automated and could produce dense point clouds, the basis for 3D surface reconstruction, and generate orthorectified mosaics, Table (2,3).

Table 2: Information about the computer's specs that processed the data

CPU	Core i7-11800HQ
RAM	32.0 GB
storage	256 SSD
GPU	NVIDIA GeForce RTX 3050

Table 3: Time and storage are used to process data.

The time of matching	43 mins 47 sec
Corresponding memory usage	7.99 GB
Time for alignment	54 mins 51 sec
Memory used for alignment	5.95 GB

The alignment includes Bundle Block Adjustment (BBA) and Aerial Triangulation (AT). At this stage, MS looks for feature points on the photos and compares them to create tie points. For each image, a sparse point cloud of tie points is recovered with an estimate of the camera's location and orientation. Twelve markers were included in MS representing GCPs, which were used for georeferencing of the models. The parameters used to build dense point clouds are illustrated in Figure (6). With Stereo Multi-View (SMV) algorithm, a high-resolution dense point cloud was created based on the sparse point cloud produced by the alignment stage.

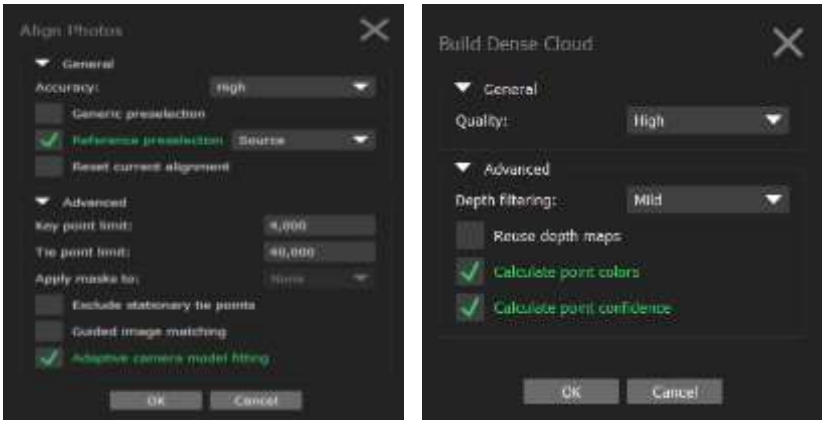

(a) **(b)**

Figure 6: In MS software, **(a)** Alignment stage settings; **(b)** MS parameters utilized in dense point cloud construction.

After this stage, the dense point clouds are ready for many options, as they are the basis for creating subsequent processing stages (such as Build Mesh and Build DEM) by editing, classifying, and exporting data for additional analysis outside the software.

- *DTM Extraction*

To generate a DTM, MS offers a feature for automatically detecting ground points based on the Adaptive Triangulated Irregular Network (ATIN) algorithm [23]. The parameters used for classifying ground points in this dataset are shown in Figure (6).

There are two steps to implementing the automated classification process; in the first stage, cells of a particular size are created from the dense cloud, and each cell's lowest point is discovered. The initial estimate of the terrain model was produced by triangulating these locations. In the second stage, the ground class gains a new point if two conditions are met: The distance to the terrain model must be within a specified range; the terrain model's angle and the line connecting this new point to a land class point must be smaller than the maximum value of the angle. The second step will be repeated if there are still some points to examine. Figure (7) shows the output from automatic classification illustrating part of the study area.

MS allows the extraction of DEMs subtracted from classified datasets, where manual editing was carefully performed after automatic classification to ensure that the based DTM is correctly computed and truly represents the terrain for further processing. Figure (8) shows DEM and DTM extracted for part of the study site. Further, the orthomosaic of the entire site was extracted automatically in MS for further inclusion in future processing.

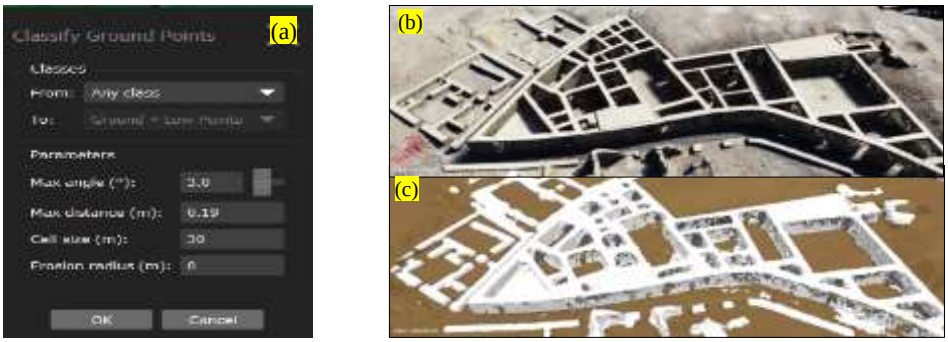

Figure 7: (a) Parameters used in automatic classification in Ur to produce ground points; (b) Part of the study area by UAV image (c) Part of the study area after applying an automatic classification algorithm of dense cloud.

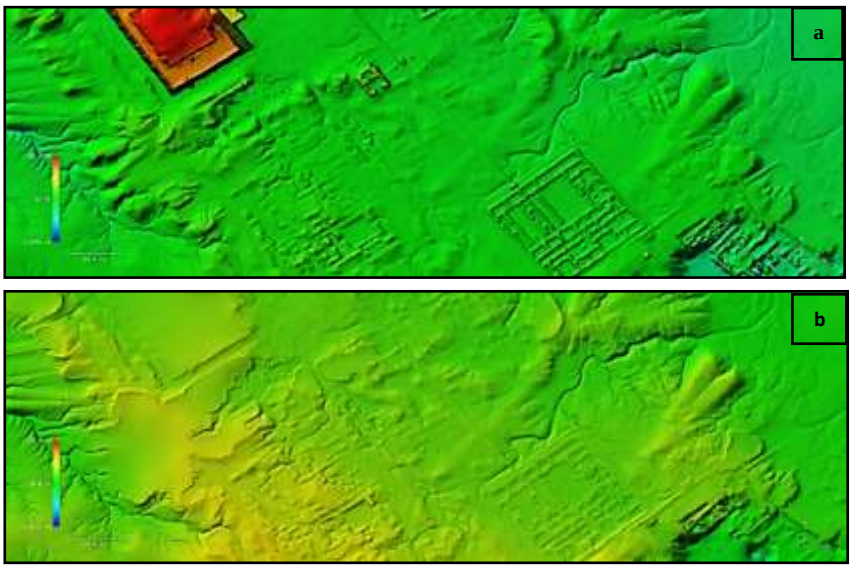

Figure 8: Part of the study area after the processing and production of models: (a) DEM and (b) DTM.

2.4. Visualization Methods (Post-Processing)

Researchers have developed various techniques for visualizing the topographic data, for being a critical step in the post-processing of the topographic mode in archeology [7], [24]–[26].

The open-source QGIS package is an advanced high-quality GIS feature with almost unparalleled depth in providing preprocessing and visualization tools included in the main package. Four visualization raster images were generated from the DTM model: Shaded relief maps (hillshade); Slope images; *Red-Relief Image Mapping* RRIM images; and Aspect images; these images represent visualization raster images. All the visualizations used add value to more understanding of the scene as no technology or single map of one size can fit all features at once [27]–[29]. This is the main power of extracting multiple visualization rasters or maps toward the possible detection of new archeological features in the site.

- *Red-Relief Image Mapping (RRIM)*

The RRIM is a method to visualize the ground surface generated by overlapping the differential openness raster with the slope raster values, which are then used to generate a combined map that shows 3D images by one image. It illustrates convexities and concavities with the topographic slope raster in red color [2], [30]. The differential openness equation (I) was applied to extract the RRIMs in the UR case study by calculating the openness coefficients, as shown in Figure (9), Equation (9), [31].

$$I = (Op - On) / 2 \quad (9)$$

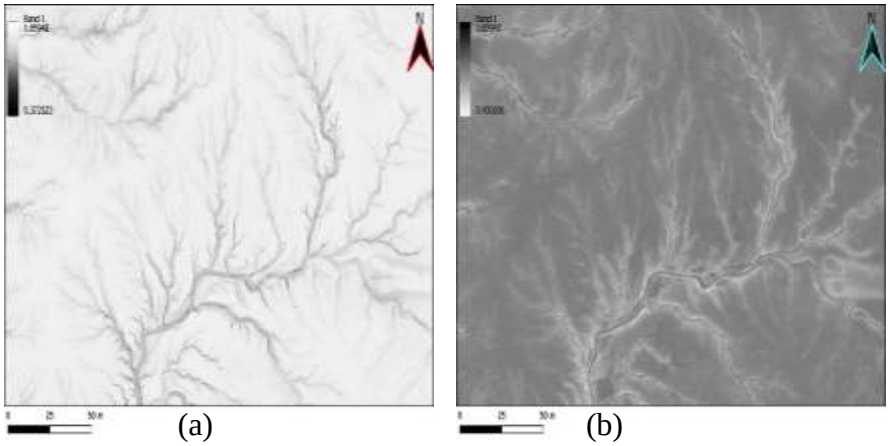

(a) (b)

Figure 9: Elements of differential openness in UR (a) Positive openness; (b) Negative.

Where the differential openness raster is (I), while Op is positive openness, and On is negative openness.

3. Results and Discussion

This section presents the results of the UAV-based photogrammetry methodology adopted in this study to detect new archeological remains in the ancient Ur city potentially. In the data acquisition stage, at the end of the flight, (7308) images were acquired after removing unwanted images to cover approximately 430 ha of the study area. At the same time, in processing results, automatic extraction and matching by powerful algorithms such as Scale-Invariant Feature Transform (SIFT) contributed to the product development of a point-dense cloud (1,088,299,187 points) derived from a separate (2,726,706 points) cloud with an RMS reprojection error (0.598241 pixels), within the SfM-MVS photogrammetry approach. The model was georeferenced through 12 ground control points listed in (MS), 4 of which were considered checkpoints to evaluate the accuracy of the produced model, Tables (4 and 5).

Table 4: Control points Root Mean Square Error (RMSE), where X= Easting, Y= Northing, Z= Altitude.

Count	X error (cm)	Y error (cm)	Z error (cm)	XY error (cm)	Total (cm)
8	0.982015	0.733701	1.15239	1.22583	1.68246

Table 5: Checkpoints RMSE, where X= Easting, Y= Northing, Z= Altitude.

Count	X error (cm)	Y error (cm)	Z error (cm)	XY error (cm)	Total (cm)
4	2.06015	1.26174	5.35365	2.41582	5.87348

The automatic 3D dense surface generation made it possible to reconstruct the DEM with an accuracy of 6.44 cm/pixel and a point density of 241 points/m2, Figure (10).

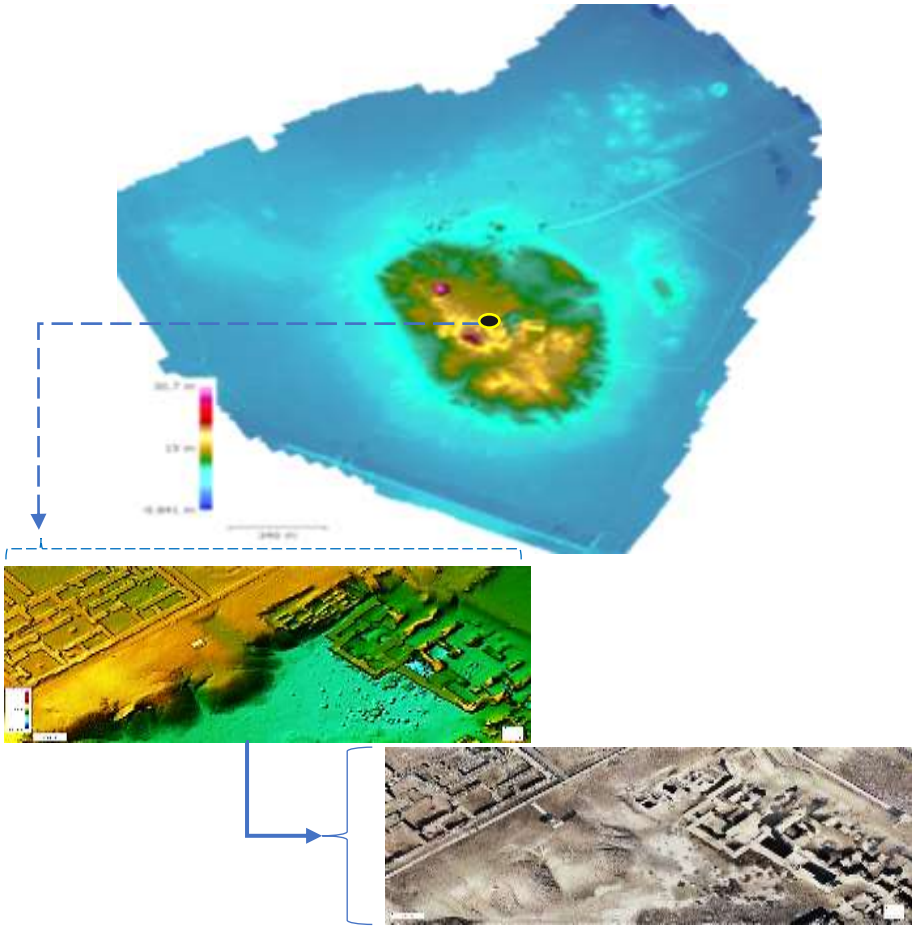

Figure 10: DEM of the ancient city of Ur by MS software.

DEM was the basis for deriving the DSM in addition to DTM by applying the Adaptive Triangulated Irregular Network (ATIN) algorithm for classifying land points, which was suitable for the topography of the study area [23].

Mosaic images were produced with a size of 82,361×96,623, colors (3 bands, uint8), and coordinate system of WGS 84 / UTM zone 38N (EPSG:32638)); Figure (11).

Figure 11: The Mosaic images of the ancient city of Ur by MS software.

On the other hand, the visual analysis techniques of the QGIS software package based on digital models derived from photogrammetry allowed the creation of two types of raster images:

1. Stand-alone raster images, hillshade raster, slope raster, aspect raster, positive and negative openness raster.
2. New hybrid raster images were created by merging multiple topographic raster layers to produce the RRIMs, which consist of merging two layers of positive openness and negative openness with a slope layer, Figure (12).

(a) (b)

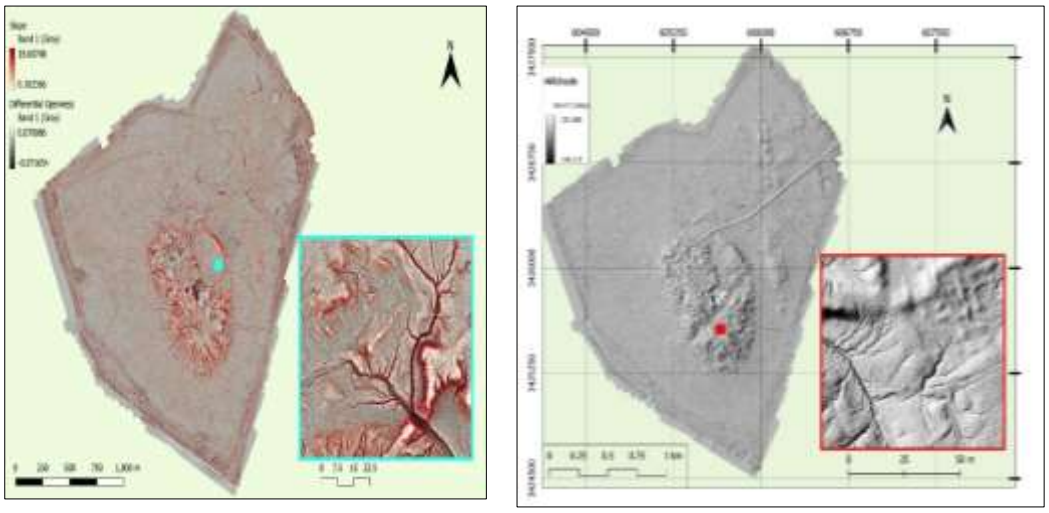

Figure 12: The ancient Ur city by QGIS software package each of (a): The RRIM layer; (b): The hillshade layer.

Through the visualization tools and techniques adopted, the archaeological features in this sector can be classified into three types: Archaeological structures, Features from previous excavations, and Possible new archaeological remains. Many buried and near-surface archaeological remains previously excavated from Woolley's campaigns left behind different types of architectural traces (such as signs of soil color difference and signs of variation in the geomorphology and topography of the study area) which allowed to identify these traces through visualization techniques applied in this study.

owever, it is noticed that all these signs share varying proportions to represent the archaeological features, so the integrated visualization techniques were found to represent an appropriate solution to overcome this limitation, taking into account the manipulation of the layer settings in each case to reach a sufficient distinction, Figure (13).

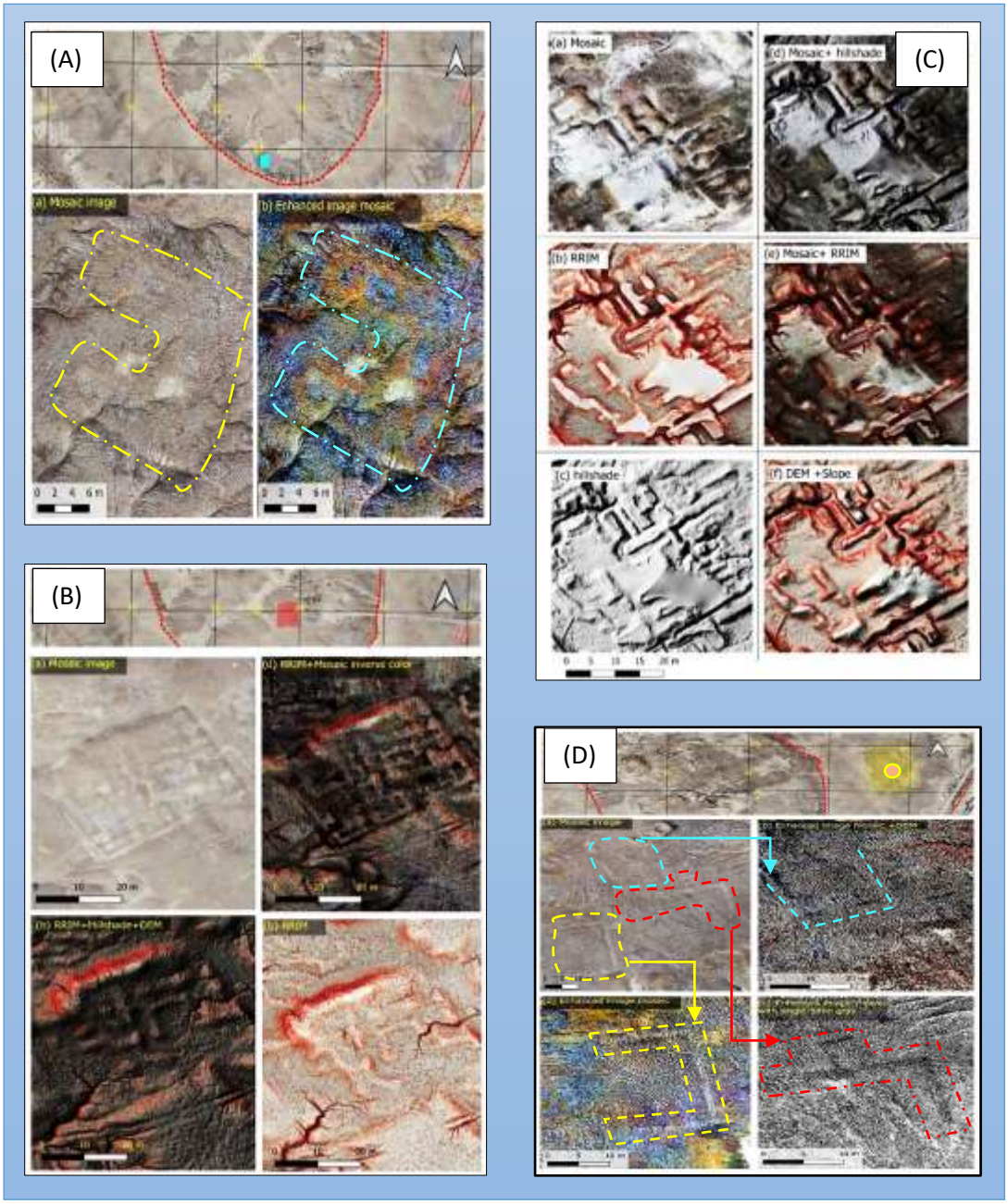

Figure 13: (A) It is located south of the hill. Markings are visible through the color of the soil. (B) It is located south of the hill, showing the topography of the previously excavated archaeological remains. (C) The archaeological features show the different visualization layers' soil color differences and terrain. (D) Some potential archaeological features south of the hill are shown with mosaic images.

After verifying the identified archaeological features by different visualization methods and by comparison with the archaeological features identified by the recent study conducted by Emily[32], a digital map was produced representing the remains of visible archaeological

structures and features from previous excavations and the potential findings of new archaeological features, Table(6), and Figure (14). Therefore, the map is a valuable digital database for researchers and specialists to analyze further and interpret the archaeological monuments in the ancient Ur City.

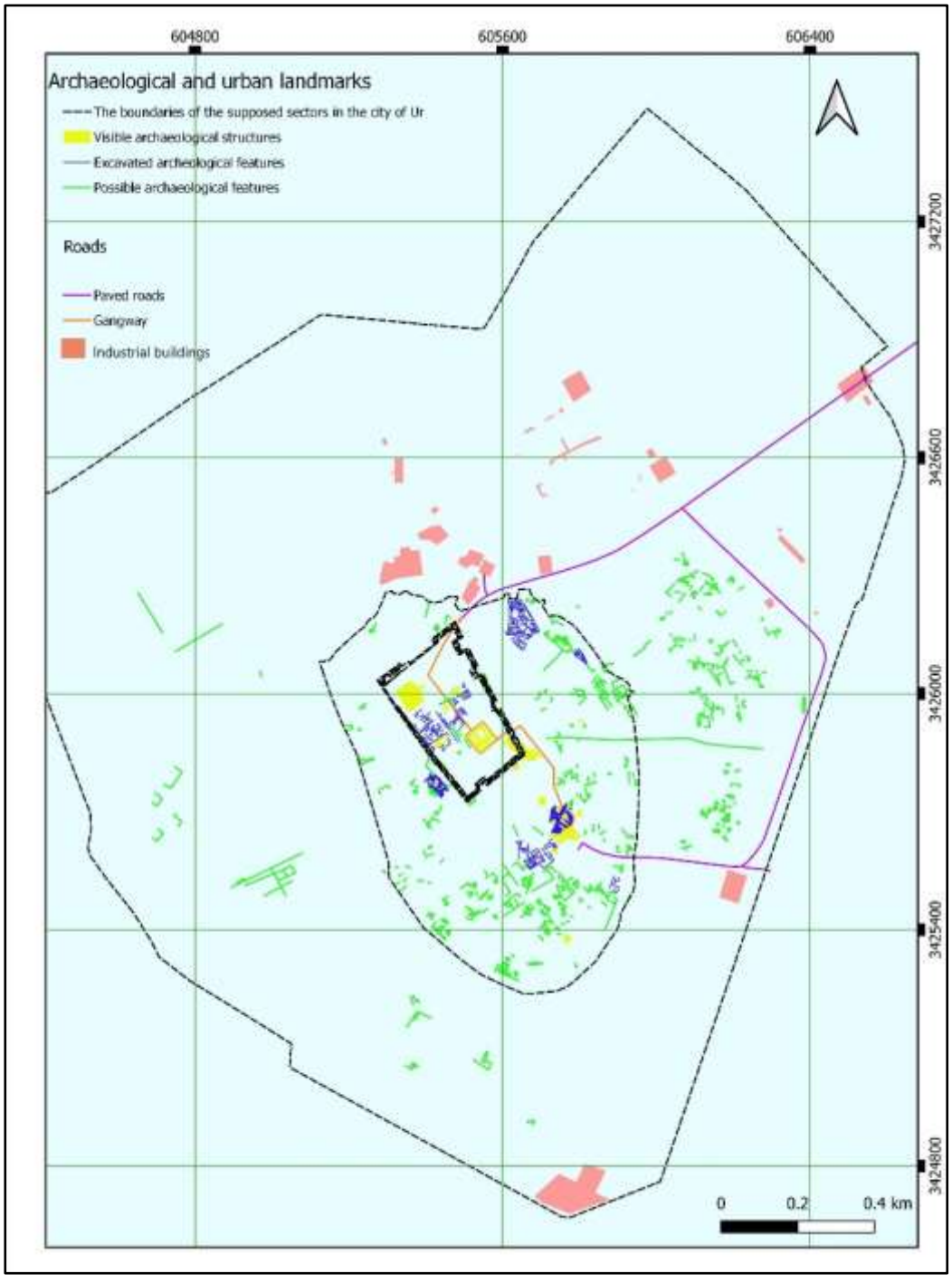

Figure 14: A digital map describing the archaeological features of the ancient Ur city was identified using visualization methods through the QGIS software.

Table 6: The surface area of possible new archaeological remains.

NO.	Sector description	Area (m2)
1	Sector A	270.07
2	Sector B	4874.27
3	Sector C	3658.94
SUM		8803.29

4. Conclusions and Recommendations

This research presented a UAV-based photogrammetry methodology following the SfM-MVS algorithms and raster image analysis to detect potential archaeological features in the ancient Ur City. This study explores the potential of RS data to improve the archeological remains detection in one of the most famous archeological sites in the world. New archeological findings were detected using standalone and integration approaches using raster analysis. Based on the methodology, visualization methods, and data analysis, several conclusions and recommendations for future work are described below.

4.1. Conclusions

The conclusions reached in this research can be summarized as follows:

1. The routine of producing 3D digital topographic models from the UAV platform using non-destructive techniques supported by AI algorithms such as SfM-MVS was beneficial in overcoming logistical and administrative hurdles during the 3D data collection process.
2. The produced topographic models can be considered as a reliable database that opens the way for the use of multiple analytical tools that have an influential role in revealing new archaeological features, modifying the ideas of settlements presented in previous studies, and documenting excavated artifacts, thus bridging the gap in traditional and destructive methods.
3. Analysis and visualization tools based on carefully selecting parameters were used to extract raster images from the 3D data provided by UAV photogrammetry. This contributed to improving the performance of the adopted standing-alone approach by effectively identifying new archaeological features at the site through the integrated approach.
4. Integrated visualization methods, by precisely defining the input parameters on the one hand and controlling the layer settings on the other hand, helped to overcome several limitations, such as the lighting effect, thus revealing new archaeological features. These methods were effective with the archaeological features characterized by signs of contrast to the terrain compared to those with signs of the architecture of contrasting soil colors.
5. The results of verifying the potential new archaeological features discovered using various visualization techniques showed that many archaeological features match Emily's maps while others have not.
6. Through the digital maps that were produced for the ancient Ur City, the shape and distribution of potential new archaeological features discovered throughout the site indicate the convergence of the geometric and architectural form of these features with the geometry of the features of the excavated monuments (width and length of the walls and their straightness and perpendicularity) that date back to the late periods of the history of Ur (such as Neo-Babylonian period, the Kishian period, and the Assyrian era).
7. This study concluded the importance of using the new UAV technology for archaeological surveys and encouraged the local authorities and the Antiquities Authority to use such technologies in their work.

4.2 Recommendations For Future Works

Some recommendations that may be useful to researchers and specialists in the future are presented below:

1. The UAV- Photogrammetric methodology used was very powerful in detecting potential archaeological features and previous excavations and documenting archaeological structures, so it could be recommended in future archaeological research alongside multi-spectral cameras to detect hidden objects better.

2. In the data processing stage, defining and strictly monitoring the parameters constraining the precision and accuracy of the produced model is recommended, especially the parameters of the automatic classification algorithm for dense cloud points in the MS software and the parameters of the RRIM construct in QGIS software. These parameters must be considered according to the site environment and the detail to be displayed.
3. Non-invasive RS methods, based on the author's knowledge, were proven their worth in detecting hidden archaeological features in the archaeological landscape, whether they are independent ones, as is the case in the methodology used in this research, or the RS fusion approach that recommend applying for future work on the archaeological site of Ur. There is a possibility to obtain information relatively more in comparison to independent RS methods and thus likely to improve data interpretation and analysis performance.

References

[1] M. Doneus, G. Mandlburger, and N. Doneus, "Archaeological ground point filtering of airborne laser scan derived point-clouds in a difficult Mediterranean environment," *J. Comput. Appl. Archaeol.*, vol. 3, no. 1, pp. 92–108, 2020, doi: 10.5334/jcaa.44.

[2] I. Kadhim and F. M. Abed, "The potential of lidar and uav-photogrammetric data analysis to interpret archaeological sites: A case study of chun castle in South-West England," *ISPRS Int. J. Geo-Information*, vol. 10, no. 1, 2021, doi: 10.3390/ijgi10010041.

[3] W. Tao, Y. Lei, and P. Mooney, "Dense point cloud extraction from UAV captured images in forest area," *ICSDM 2011 - Proc. 2011 IEEE Int. Conf. Spat. Data Min. Geogr. Knowl. Serv.*, pp. 389–392, 2011, doi: 10.1109/ICSDM.2011.5969071.

[4] I. Kadhim and F. Abed, "Investigating the old city of Babylon: tracing buried structural history based on photogrammetry and integrated approaches," no. October, p. 9, 2021, doi: 10.1117/12.2597696.

[5] Ž. Kokalj and M. Somrak, "Why not a single image? Combining visualizations to facilitate fieldwork and on-screen mapping," *Remote Sens.*, vol. 11, no. 7, 2019, doi: 10.3390/rs11070747.

[6] P. J. Kennelly, "Terrain maps displaying hill-shading with curvature," *Geomorphology*, vol. 102, no. 3–4, pp. 567–577, 2008, doi: 10.1016/j.geomorph.2008.05.046.

[7] K. Millard, C. Burke, D. Stiff, and A. Redden, "Detection of a low-relief 18th-century British siege trench using LiDAR vegetation penetration capabilities at Fort Beauséjour-Fort Cumberland National Historic Site, Canada," *Geoarchaeology*, vol. 24, no. 5, pp. 576–588, 2009, doi: 10.1002/gea.20281.

[8] M. Doneus, "Openness as visualization technique for interpretative mapping of airborne lidar derived digital terrain models," *Remote Sens.*, vol. 5, no. 12, pp. 6427–6442, 2013, doi: 10.3390/rs5126427.

[9] D. S. Davis, M. C. Sanger, and C. P. Lipo, "Automated mound detection using lidar and object-based image analysis in Beaufort County, South Carolina," *Southeast. Archaeol.*, vol. 38, no. 1, pp. 23–37, 2019, doi: 10.1080/0734578X.2018.1482186.

[10] A. Qubaa and S. Al-Hamdani, "Detecting abuses in archaeological areas using k-mean clustering analysis and UAVs/drones data," *Sci. Rev. Eng. Environ. Sci.*, vol. 30, no. 1, pp. 182–194, 2021, doi: 10.22630/PNIKS.2021.30.1.16.

[11] A. R. Qubaa, A. N. Hamdon, and T. A. Al Jawwadi, "Morphology Detection in Archaeological Ancient Sites by Using UAVs/Drones Data and GIS techniques," *Iraqi J. Sci.*, vol. 62, no. 11, pp. 4557–4570, 2021, doi: 10.24996/ijs.2021.62.11(SI).35.

[12] M. Dubbini, L. I. Curzio, and A. Campedelli, "Digital elevation models from unmanned aerial vehicle surveys for archaeological interpretation of terrain anomalies: Case study of the Roman castrum of Burnum (Croatia)," *J. Archaeol. Sci. Reports*, vol. 8, pp. 121–134, 2016, doi: 10.1016/j.jasrep.2016.05.054.

[13] A. Abdelhafiz, *Integrating Digital photogrammetry integrating digital photogrammetry and terrestrial laser scanning*, no. 631. 2009.

[14] H. Crawford, "*Ur The City of the Moon God,"* vol. 12, no. 2007. 2014.

[15] R. M. Rowlett and R. M. Adams, "*Heartland of Cities,"* vol. 24, no. 3. 1983.

[16] M. R. R. El Meouchea, I. Hijazi, PA Poncet, M. Abunemeh, "UAV Photogrammetry Implementation to Enhance Land Surveying, Comparisons and Possibilities," vol. XLII, no. October, pp. 20–21, 2016, doi: 10.5194/isprs-archives-XLII-2-W2-107-2016.

[17] S. Kerner, I. Kaufman, and Y. Raizman, "Role of tie-points distribution in aerial photography," *Int. Arch. Photogramm. Remote Sens. Spat. Inf. Sci. - ISPRS Arch.*, vol. 40, no. 3W4, pp. 41–44, 2016, doi: 10.5194/isprsarchives-XL-3-W4-41-2016.

[18] K. N. Tahar, "An evaluation on different number of ground control points in unmanned aerial vehicle photogrammetric block," *Int. Arch. Photogramm. Remote Sens. Spat. Inf. Sci. - ISPRS Arch.*, vol. XL-2/W2, no. November, pp. 93–98, 2013, doi: 10.5194/isprsarchives-XL-2-W2-93-2013.

[19] S. I. Jiménez-Jiménez, W. Ojeda-Bustamante, M. D. J. Marcial-Pablo, and J. Enciso, "Digital terrain models generated with low-cost UAV photogrammetry: Methodology and accuracy," *ISPRS Int. J. Geo-Information*, vol. 10, no. 5, 2021, doi: 10.3390/ijgi10050285.

[20] H. H. Ali and F. M. Abed, "The impact of UAV flight planning parameters on topographic mapping quality control," *IOP Conf. Ser. Mater. Sci. Eng.*, vol. 518, no. 2, 2019, doi: 10.1088/1757-899X/518/2/022018.

[21] P. R. Wolf, B. A. Dewitt, and B. E. Wilkinson, *Elements of Photogrammetry with Application in GIS*, vol. 110, no. 9. 2016.

[22] J. M. Gómez-López, J. L. Pérez-García, A. T. Mozas-Calvache, and J. Delgado-García, "Mission flight planning of rpas for photogrammetric studies in complex scenes," *ISPRS Int. J. Geo-Information*, vol. 9, no. 6, 2020, doi: 10.3390/ijgi9060392.

[23] P. Klápště, M. Fogl, V. Barták, K. Gdulová, R. Urban, and V. Moudrý, "Sensitivity analysis of parameters and contrasting performance of ground filtering algorithms with UAV photogrammetry-based and LiDAR point clouds," *Int. J. Digit. Earth*, vol. 0, no. 0, pp. 1672–1694, 2020, doi: 10.1080/17538947.2020.1791267.

[24] B. J. Devereux, G. S. Amable, and P. Crow, "Visualisation of LiDAR terrain models for archaeological feature detection," *Antiquity*, vol. 82, no. 316, pp. 470–479, 2008, doi: 10.1017/S0003598X00096952.

[25] J. M. Harmon, M. P. Leone, S. D. Prince, and M. Snyder, "LiDAR for Archaeological Landscape Analysis: A Case Study of Two Eighteenth-Century Maryland Plantation Sites," *Am. Antiq.*, vol. 71, no. 4, pp. 649–670, 2006, doi: 10.2307/40035883.

[26] B. Štular, Ž. Kokalj, K. Oštir, and L. Nuninger, "Visualization of lidar-derived relief models for detection of archaeological features," *J. Archaeol. Sci.*, vol. 39, no. 11, pp. 3354–3360, 2012, doi: 10.1016/j.jas.2012.05.029.

[27] J. C. Fernandez-Diaz, W. E. Carter, R. L. Shrestha, and C. L. Glennie, "Now you see it...

Now you don't: Understanding airborne mapping LiDAR collection and data product generation for archaeological research in Mesoamerica," *Remote Sens.*, vol. 6, no. 10, pp. 9951–10001, 2014, doi: 10.3390/rs6109951.

[28] K. Challis, P. Forlin, and M. Kincey, "A generic toolkit for the visualization of archaeological features on airborne LiDAR elevation data," *Archaeol. Prospect.*, vol. 18, no. 4, pp. 279–289, 2011, doi: 10.1002/arp.421.

[29] R. Bennett, K. Welham, R. A. Hill, and A. Ford, "A comparison of visualization techniques for models created from airborne laser scanned data," *Archaeol. Prospect.*, vol. 19, no. 1, pp. 41–48, 2012, doi: 10.1002/arp.1414.

[30] J. Tzvetkov, "Relief visualization techniques using free and open source GIS tools," *Polish Cartogr. Rev.*, vol. 50, no. 2, pp. 61–71, 2018, doi: 10.2478/pcr-2018-0004.

[31] R. Yokoyama, M. Shirasawa, and R. J. Pike, "Visualizing topography by openness: A new application of image processing to digital elevation models," *Photogramm. Eng. Remote Sensing*, vol. 68, no. 3, pp. 257–265, 2002.

[32] E. Hammer, "the City and Landscape of Ur: an Aerial, Satellite, and Ground Reassessment," *Iraq*, vol. 81, pp. 173–206, 2019, doi: 10.1017/irq.2019.7.